



## Research article

# Improving the thermostability of *Trichoderma reesei* xylanase 2 by introducing disulfide bonds



Feng Tang, Daiwen Chen, Bing Yu, Yuheng Luo, Ping Zheng, Xiangbing Mao, Jie Yu, Jun He \*

<sup>a</sup> Institute of Animal Nutrition, Sichuan Agricultural University, Chengdu, Sichuan 611130, People's Republic of China

<sup>b</sup> Key Laboratory of Animal Disease-Resistance Nutrition, Ministry of Education, Beijing, People's Republic of China

## ARTICLE INFO

## Article history:

Received 6 November 2016

Accepted 9 January 2017

Available online 12 January 2017

## Keywords:

Disulfide bond introduction

Feed pelleting

Glycoside hydrolase

Industry applications

Pulp bleaching

Site-directed mutagenesis

Stable xylanase

Xylan degradation

Xylanolytic enzymes

## ABSTRACT

**Background:** Xylanases are considered one of the most important enzymes in many industries. However, their low thermostability hampers their applications in feed pelleting, pulp bleaching, and so on. The main aim of this work was to improve the thermostability of *Trichoderma reesei* xylanase 2 (Xyn2) by introducing disulfide bonds between the N-terminal and  $\alpha$ -helix and the  $\beta$ -sheet core.

**Results:** In this work, two disulfide bonds were separately introduced in the Xyn2 to connect the N-terminal and  $\alpha$ -helix to the  $\beta$ -sheet core of Xyn2. The two disulfide bonds were introduced by site-directed mutagenesis of the corresponding residues. The half-life of the mutants Xyn2<sup>C14–52</sup> (disulfide bond between  $\beta$ -sheets B2 and B3) and Xyn2<sup>C59–149</sup> (disulfide bond between  $\beta$ -sheets A5 and A6) at 60°C was improved by approximately 2.5- and 1.8-fold compared to that of the wild type Xyn2. In addition, the enzyme's resistance to alkali and acid was enhanced.

**Conclusion:** Our results indicated that the connection of the N-terminal and  $\alpha$ -helix to the  $\beta$ -sheet core is due to the stable structure of the entire protein.

© 2017 Pontificia Universidad Católica de Valparaíso. Production and hosting by Elsevier B.V. All rights reserved. This is an open access article under the CC BY-NC-ND license (<http://creativecommons.org/licenses/by-nc-nd/4.0/>).

## 1. Introduction

Xylan mainly consists of D-xyloses connected by  $\beta$ -1,4-D-linkage and is the major constituent of hemicellulose in cells and the second-most abundant polysaccharide in nature [1]. There are several xylanolytic enzymes involved in the complete degradation procedure of xylan because of its complex structure. Endo- $\beta$ -1,4-D-xylanases play a key role in the hydrolysis of xylan because of their ability to cleave the internal  $\beta$ -1,4-D-xylosidic linkages, which are the main linkages in xylan [2]. In the last few decades, xylanase has attracted much attention because of its wide industrial applications in food technology, feed technology, and pulp industry, and it has even been used in biofuel production [3,4,5,6]. Xylanases have been primarily classified into glycoside hydrolase (GH) family 5, 8, 10, 11, 30, and 43 according to the hydrophobic cluster analysis of the catalytic domains and similarities in the amino acid sequences [7]. Among these, GH family 11 xylanases have gained much attention because of their high substrate selectivity, high catalytic efficiency, and a relatively simple

structure that mainly consists of an  $\alpha$ -helix and two  $\beta$ -sheets packed against each other [8].

However, most naturally isolated enzymes are not competent for industrial applications because of their low thermostability, acid (or alkali) resistance, and so on [2,9,10]. Although thermostable xylanase can be isolated from natural thermophiles such as *Thermotoga maritime* (producing XynA and XynB), their low specific activity and contamination of other side activities limits their use [11,12].

Improving the thermal properties of mesophilic xylanases through genetic engineering is considered an effective approach to obtaining thermostable xylanases [10,13]. Introduction of a disulfide bond is the most efficient method for improving the stability of a protein and has been widely used in many other proteins [14,15,16]. Previous studies on xylanases indicated that the  $\beta$ -sheet core is a stable structure of GH family 11 xylanases. Moreover, the N-terminal, C-terminal, and  $\alpha$ -helix are the most notable differences between thermophilic and mesophilic xylanases [17,18,19,20]. In addition, many studies have successfully improved the thermostability of mesophilic xylanases by connecting the N-terminal, C-terminal, or  $\alpha$ -helix [17,21,22,23,24,25]. However, the connection between the N-terminal, C-terminal, and  $\alpha$ -helix and the  $\beta$ -sheet core was barely mentioned in previous studies.

The endo-1,4- $\beta$ -xylanase 2 (Xyn2) of *Trichoderma reesei* is one of the most important xylanases used in industry [26]. It is a

\* Corresponding author.

E-mail address: [hejun8067@163.com](mailto:hejun8067@163.com) (J. He).

Peer review under responsibility of Pontificia Universidad Católica de Valparaíso.

low-molecular-mass (20 kDa) enzyme with an alkaline isoelectric point (pI 9.0) and activity optimum at pH 4–6. However, the temperature optimum of *T. reesei* Xyn2 is approximately 50–55°C, and it cannot withstand temperatures above 65°C, the most common temperature range in industrial applications [18,27]. Therefore, in this work, we aimed to improve the thermostability of Xyn2 through protein engineering. Previous studies have implicated the role of disulfide bond in the determination of thermostability; we accordingly designed amino acid mutations in the N-terminal and C-terminal of *T. reesei* Xyn2. Our aim was to increase the thermostability of Xyn2 by introducing disulfide bonds between the unstable regions (N-terminal and  $\alpha$ -helix) and the stable core ( $\beta$ -sheet core).

## 2. Materials and methods

### 2.1. Vector, microbial strains, and culture media

*T. reesei* Rut C-30 (Mutated type, ATCC56765) preserved in laboratory was used as the Xyn2 gene donor (GenBank Accession No. EU532196.1). *Escherichia coli* (TianGen CB101) and vector pMD19-T (Takara D104A) were used for gene cloning, and *E. coli* Origami (DE3) and vector pET32a were used for expression. *T. reesei* Rut C-30 was cultured in a basal medium (61% tryptone, 0.3% yeast extract) for the expression of the Xyn2 gene. *E. coli* DH5 $\alpha$  and Origami (DE3) were cultured at 37°C in Luria–Bertani medium containing 100  $\mu$ g/mL Amp for selection.

### 2.2. Cloning of Xyn2 from *T. reesei*

Spores of *T. reesei* Rut C-30 (100  $\mu$ L) were inoculated in 100 mL of basal medium and cultured at 28°C for 48 h. Then the fungal mycelia were harvested for total RNA isolation using RNAsiso Plus (Takara D312) as described previously [28]. The first strand cDNA was synthesized with 500 ng of total RNA using Prime Script II 1st Strand cDNA Synthesis Kit (Takara) according to the manufacturer's instructions. The protein-coding sequence of *T. reesei* Xyn2 (GenBank Accession No. EU532196.1) was amplified by a pair of primers, F1 (5'-GCTGAATTCAGACGATTCAGCCCGCA-3') and R1 (5'-ATGCGCCGCTTACGTGACGGTGATGGAA-3'), supplied with the restriction sites *Eco*RI and *Not*I, respectively. The PCR fragments were ligated to pMD19-T (Simple) vector (Takara) by TA cloning, and the recombinant cloning vector was named pMD19T-Xyn2. The *T. reesei* Xyn2 genes were sequenced by Sangon Biotech Co. and corrected by DNAMAN 6.0 (<http://www.lynnon.com>) with the template from GenBank (National Center for Biotechnology Information, <http://www.ncbi.nlm.nih.gov/nucleotide/EU532196.1>).

**Table 1**

Primers for mutants.

Enzyme <sup>a</sup>	Mutant site <sup>b</sup>	Primers <sup>c</sup>
Xyn2 <sup>C14–52</sup>	F14C	5'-CGTTCAGTACGAGTAGCAGTAGCCGTGTG-3' 5'-GCTACTCGTACTGGAACGATGGCCACGGC-3'
	Q52C	5'-TCTGGTGCCGGACACCATCCCTTGGC-3' 5'-CGGCAAGGGATGGTGTCCCGGACCAAGA-3'
Xyn2 <sup>C59–149</sup>	V59C	5'-CTGCCGAGAAGTTGATGCACTTGTCTTGGTGCCGG-3' 5'-TGCATCACTTCTCGGCACTACAACCCCAACGG-3'
	S149C	5'-GTTCCGGTGTGACAGCGCCGCTCAGC-3' 5'-CGTCAACACGGCGAACCCTCAACCGGTGG-3'

<sup>a</sup> The mutant enzymes Xyn2<sup>C14–52</sup> and Xyn2<sup>C59–149</sup> contain two mutations F14C, Q52C and V59C, S149C respectively.

<sup>b</sup> The introduced mutations in this study are underlined.

<sup>c</sup> All the mutation sites in the primers are underlined.

### 2.3. Mutagenesis of Xyn2 gene

Each mutant of Xyn2<sup>C14–52</sup> and Xyn2<sup>C59–149</sup> were separately constructed with a pair of primers (Table 1) using the Fast Mutagenesis System Kit (TransGen Biotech Co, FM111-01) according to the manufacturer's instructions. The nucleic acid sequence of the mutants was identified by sequencing (Sangon Co, Shanghai) and confirmed by DNAMAN6.0.

### 2.4. Prediction of the crystal structure of Xyn2 and its mutants

A homologous crystal structure (PDB code: 3akq) that was fully identical to the amino acid sequence of the wild type *T. reesei* Rut C-30 Xyn2 was chosen as the template model for mutants. The three-dimensional crystal structure of the mutants was modeled using Swiss PDB Viewer 4.1 (<http://spdbv.vital-it.ch>) with Swiss Model programs based on the coordinates of the PDB code 3akq. The final coordinates of the mutants were calculated using the energy minimization program.

### 2.5. Expression and purification of Xyn2 and its mutants

All the Xylanase genes Xyn2, Xyn2<sup>C14–52</sup>, and Xyn2<sup>C59–149</sup> located in the recombinant cloning vector were digested by *Eco*RI (Takara Code: 1611) and *Not*I (Takara Code: 1623) and ligated to pET32a(+) having the corresponding sticky ends. Recombinant vectors with the wild and mutant genes were then transformed into *E. coli* Origami (DE3) cells and induced by 0.1% IPTG. The cells were then harvested by centrifugation at 10,000  $\times$  g at 4°C for 5 min. The cells were lysed by 0.1 mg/mL lysozyme, and the supernatant (soluble protein) was harvested by centrifugation at 10,000  $\times$  g at 4°C for 10 min. The supernatant (crude enzymes) was removed and directly loaded onto a 2-mL Ni<sup>2+</sup>-chelating chromatography column according to the instruction manual (Bio-Rad, USA) and subsequently eluted with an elution buffer (300 mM NaCl, 50 mM sodium phosphate, and 500 mM imidazole, pH 8.0).

### 2.6. Mass spectrometry

The samples were analyzed by matrix-assisted laser desorption/ionization time-of-flight/time-of-flight mass spectrometry (MALDI-TOF-TOF-MS) performed by BGI Tech., China (<http://www.bgitechsolutions.com>). Spectra were acquired using the enhanced scanning mode covering a mass range of m/z 500–3500 with a distinguishability of 50,000. Database searches using the peak list files of the processed mass spectra were performed using Mascot 2.3.02 (<http://www.matrixscience.com>) and UniProt *T. reesei* database ([http://www.uniprot.org/taxonomy/?query=Trichoderma\\_reesei&sort=score](http://www.uniprot.org/taxonomy/?query=Trichoderma_reesei&sort=score)).

### 2.7. Enzyme activity and protein assays

The activity of the endo-1,4- $\beta$ -xylanases was determined colorimetrically by a standard procedure using 3,5-dinitrosalicylic acid (DNS), as described by Zhang [29]. In brief, 40  $\mu$ L of enzyme diluted with McIlvaine buffer (0.2 M sodium phosphate, 0.1 M citric acid, pH 6.0) was added to 360  $\mu$ L of 1% (w/v) beech wood xylan, which was suspended in the same buffer, and incubated at 50°C for 10 min. The reducing sugars hydrolyzed by xylanase were developed by the developer 600  $\mu$ L of DNS after boiling at 100°C for 10 min. The absorbance of the solution was then measured at 540 nm using a visible-spectrophotometer. In the control experimental group, xylanase was added in the last step. One unit (IU) of xylanase activity was defined as the amount of enzyme liberating 1  $\mu$ mol of reducing sugar equivalent per minute.

The total protein produced by the induced and noninduced *E. coli* Origami (DE3) with the pET32a(+) expression vector and recombinant expression vectors was detected on 12% (w/v) SDS-PAGE after boiling for 5 min in the presence of 5%  $\beta$ -mercaptoethanol. The proteins were then visualized by Coomassie brilliant blue R 250 staining. The protein concentration was determined by the Bradford method using bovine serum albumin as the standard.

### 2.8. Validation of the formation of disulfide bonds

The formation of disulfide bonds was determined by the method described by Wakarchuk [30]. In brief, the wild enzyme (control) and mutants were pretreated with a gradient concentration of dithiothreitol (DTT) from 1 to 5 mM in the presence of 1% SDS at 70°C for 5 min and then separated on 12% (w/v) SDS-PAGE.

To evaluate whether the increasing thermostability of the mutants resulted from the introduction of a disulfide bond, the purified protein was evaluated by the method described by Yang [24]. In brief, the mutants and wild type xylanases were treated with 10 mM DDT at 4°C for 12 h; untreated enzyme was used as the control. The residual activities of Xyn2 and the mutants (Xyn2<sup>C14-52</sup> and Xyn2<sup>C59-149</sup>) treated with 10 mM DDT or untreated were measured by a standard procedure after incubation at 60°C for 10 min. The results were calculated as enzyme activity relative to the nonincubated enzymes.

### 2.9. Measurement of optimal pH for activity and stability

The pH optimum of each enzyme was determined by incubating the xylanases with 1.0% beech wood xylan substrate at 50°C for 10 min in a range of pH from 2.0 to 8.0 in the 100 mM Mcllvaine buffer mentioned above and pH from 9.0 to 10.0 in 50 mM glycine-NaOH buffer (0.2 M

NaOH, 0.05 M Glycine) [15]. The pH condition that exhibited the highest activity was determined as the optimal pH.

The pH stability of each enzyme was determined by assaying their residual activity at the standard conditions mentioned above after preincubation at 60°C for 10 min in the pH range 2.0–10.0 without the beech wood xylan substrate [24]. The buffers for the different pHs were 100 mM Mcllvaine buffer (pH 2.0–8.0) and 50 mM glycine-NaOH (pH 9.0–10.0), as mentioned above.

### 2.10. Measurement of optimal temperature and thermostability

The temperature optimum of each enzyme was determined by incubating xylanases in 50 mM Mcllvaine buffer (pH 6.0) with 1.0% xylan substrate in the temperature range 30–80°C, and the highest activity in the temperature condition was determined as the optimal temperature.

The thermostability of the xylanases was measured by incubating the xylanases in 50 mM pH 6.0 Mcllvaine buffer without the beech wood xylan substrate for 10 min at temperatures in the range 50–80°C, and the residual activities were measured by a standard assay procedure after cooling on ice; the control was placed on ice without pretreatment.

### 2.11. Determination of kinetic parameters of Xyn2 and its mutants

Determining the  $K_m$  and  $V_{max}$  of Xyn2 and its mutants was performed by mixing 40  $\mu$ L of diluted enzyme with 360  $\mu$ L beech wood xylan with a gradient concentration of 0.125–2.0% (w/v) by the standard procedure described above. The values of  $K_m$  and  $V_{max}$  were determined according to the Michaelis–Menten equation using a Lineweaver–Burk plot.

The xylanases were incubated in Mcllvaine buffer, pH 6.0, at 60°C, and the residual activity was measured at every indicated period (1, 3, 5, 10, 15, 20, and 30 min) to determine the half-life ( $t_{1/2}$ ) of Xyn2 and its mutants in high-temperature condition. The half-life was

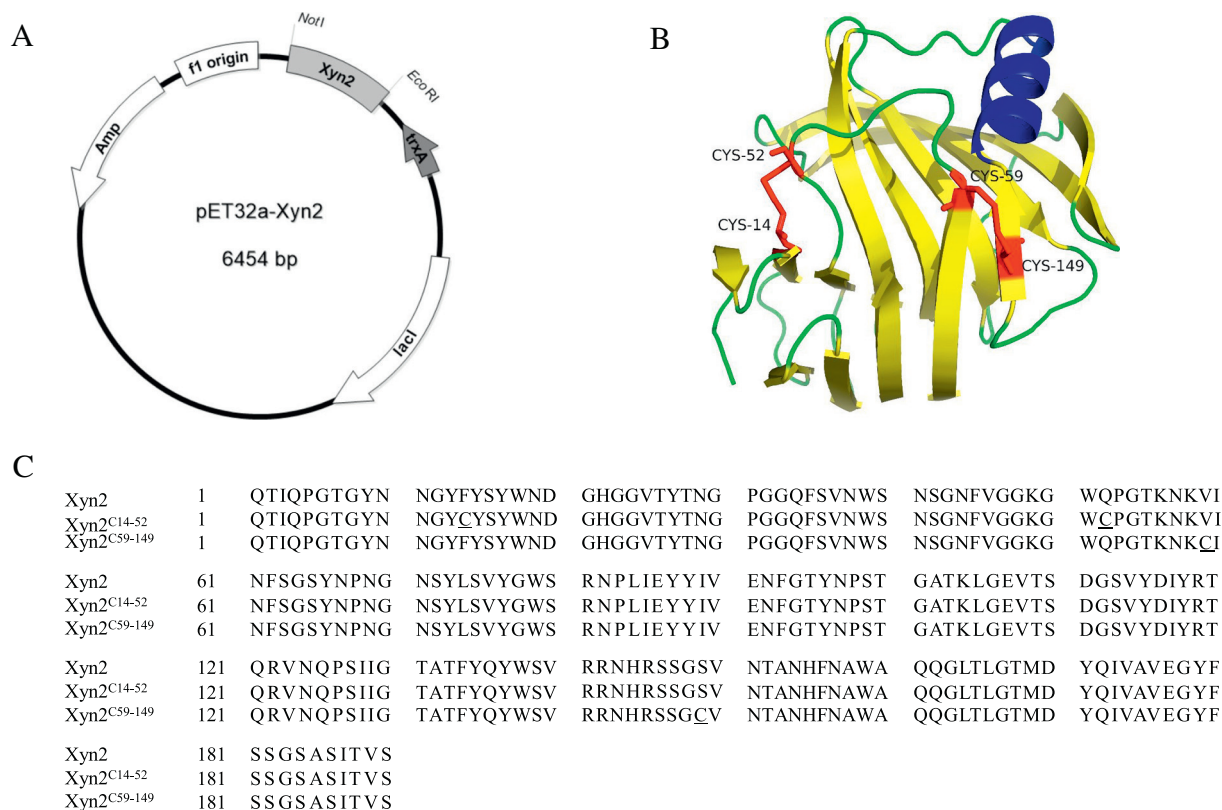


**Fig. 1.** Construction of Xyn2 and its mutants. (A) A recombinant expression vector. (B) A superimposed three-dimensional structures of the disulfide bond in Xyn2; (C) Amino acid sequence alignment of Xyn2 and its mutants; mutant amino acid residues are underlined.

calculated using the equation  $y = A * e^{-kt}$ , which was fitted to specific activity–time curves with Excel and the  $t_{1/2}$  was equal to  $\ln 2/k$  [24].

### 3. Results

#### 3.1. Cloning of *T. reesei* Xyn2 and its mutated genes

The *T. reesei* Xyn2 gene, approximately 573 bp in length, was amplified from first strand cDNA prepared from *T. reesei* using a pair of primers. The specific PCR product, approximately 600 bp, was observed by agarose gel electrophoresis and ligated into the cloning vector pMD19-T by TA cloning. The recombinant vector pMD19T-Xyn2 was confirmed by subsequent sequencing with the primer M13–47 (Sangon tech, <http://www.sangon.com/index.jsp>). The results indicated that the Xyn2 gene was successfully integrated into the vector pMD19-T, and the nucleotide sequences fully matched that of *T. reesei* Rut C-30 Xyn2 (GenBank Accession No. EU532196.1).

Two specific primers (F1 and R1) each containing a restriction enzyme site *Eco*RI and *Not*I, respectively, allowed the directional cloning of the Xyn2 gene from pMD19T-Xyn2 into the pET32a expression vector. The recombinant expression vector pET32a-Xyn2 was confirmed by sequencing with the primer S-Tag (Sangon tech, <http://www.sangon.com/index.jsp>). The Xyn2 gene and its mutants were designed to be expressed coupled with the *trxA* gene to form the disulfide bond in *E. coli* (Fig. 1A).

Mutagenesis of F14C, Q52C, V59C, and S149C was performed by a pair of mutant primers using the template of the vector pET3a-Xyn2 and was confirmed by sequencing. In addition, the mutant recombinant vectors pET32a-Xyn2<sup>C14–52</sup> (containing mutant sites F14C and Q52C) and pET32a-Xyn2<sup>C59–149</sup> (containing mutant sites V59C and S149C) were fully matched to the target nucleotide sequences. The mutant amino acid residues are highlighted in Fig. 1C with an underline. The three-dimensional structure of the mutants was predicted by Swiss PDB Viewer 4.1 (<http://spdbv.vital-it.ch>) based on the coordinates of the PDB code 3akq (RCSB Protein Data Bank, <http://www.rcsb.org/pdb/explore/explore.do?structureId=3akq>). The disulfide bonds of Cys<sup>14–52</sup> and Cys<sup>59–149</sup> are demonstrated in Fig. 1B.

#### 3.2. Expression and purification of Xyn2 and its mutated genes

The *E. coli* Origami (DE3) transformants pET3a-Xyn2, pET32a-Xyn2<sup>C14–52</sup>, and pET32a-Xyn2<sup>C59–149</sup> were used for inducible expression with 0.1% IPTG. The total protein of the induced and non-induced transformants was collected and visualized on 12%

**Table 2**  
Results for mass spectrometry.

Sample name	Protein ID <sup>a</sup>	Mascot score	Coverage rate	Pep Count	E-value
Xyn2	tr B2CNY5 B2CNY5_HYPJE	145	42.11%	5	0.00000
Xyn2 <sup>C14–52</sup>	tr B2CNY5 B2CNY5_HYPJE	151	45.79%	5	0.00000
Xyn2 <sup>C59–149</sup>	tr B2CNY5 B2CNY5_HYPJE	151	44.39%	5	0.00000

<sup>a</sup> From the UniProt *T. reesei* Database: [http://www.uniprot.org/taxonomy/?query=Trichoderma\\_reesei&sort=score](http://www.uniprot.org/taxonomy/?query=Trichoderma_reesei&sort=score)

SDS-PAGE. As expected, the total protein of the induced *E. coli* Origami was much more than that of the noninduced cells at the molecular mass 37 kDa; this was similar to the calculated size (Fig. 2A).

The crude enzymes were purified by Ni<sup>2+</sup>-NTA affinity chromatography and subsequently identified by MALDI-TOF-TOF-MS; MALDI-TOF-TOF-MS results of Xyn2 are shown in Fig. 2B (MS results for Xyn2<sup>C14–52</sup> and Xyn2<sup>C59–149</sup> are shown in supplementary files). The purified enzymes mostly matched the *T. reesei* Rut C-30 Xyn2 (the strain used in this work) with a similarity rate of above 40% (Table 2), indicating that the proteins expressed by *E. coli* Origami (DE3) were either *T. reesei* xylanases or its mutants.

#### 3.3. Validation of the disulfide bonds

The formation of disulfide bonds in Xyn2<sup>C14–52</sup> and Xyn2<sup>C59–149</sup> was predicted by Swiss PDB viewer and verified by the method described by Yang [24]. In brief, the xylanases were pretreated with 0–5 mM DDT and boiled at 70°C for 5 min prior to SDS-PAGE. The presence of disulfide bonds changed the mobility of the protein in SDS-PAGE. Enzymes that do not contain a disulfide bond tend to bind more to SDS and thus migrate slower than the enzymes with an intact disulfide bond. In the presence of 1 mM DTT, the Xyn2<sup>C14–52</sup> and Xyn2<sup>C59–149</sup> mutants displayed two bands in 12% SDS-PAGE (Fig. 3A, lanes 5 and 8). Xyn2<sup>C14–52</sup> and Xyn2<sup>C59–149</sup> migrated slower when the concentration of DTT rose to 10 mM because of the reduction of the disulfide bond (Fig. 3A, lanes 6 and 9). However, the wild type displayed no mobility difference in the presence or absence of DTT (Fig. 3A, lanes 1–3).

After treatment with 10 mM DDT at 4°C for 12 h, the wild type enzymes were treated by the same procedure as the control, as described by Yang [24]. The respective residual activities of Xyn2<sup>C14–52</sup> and Xyn2<sup>C59–149</sup> at 60°C for 10 min decreased to 9.8 and 31.6%, which is significantly ( $P < 0.05$ ) lower than that of the untreated mutants, but DDT-treated Xyn2 retained almost the same residual activity as the untreated enzyme at 60°C for 10 min (Fig. 3B). It indicates that the

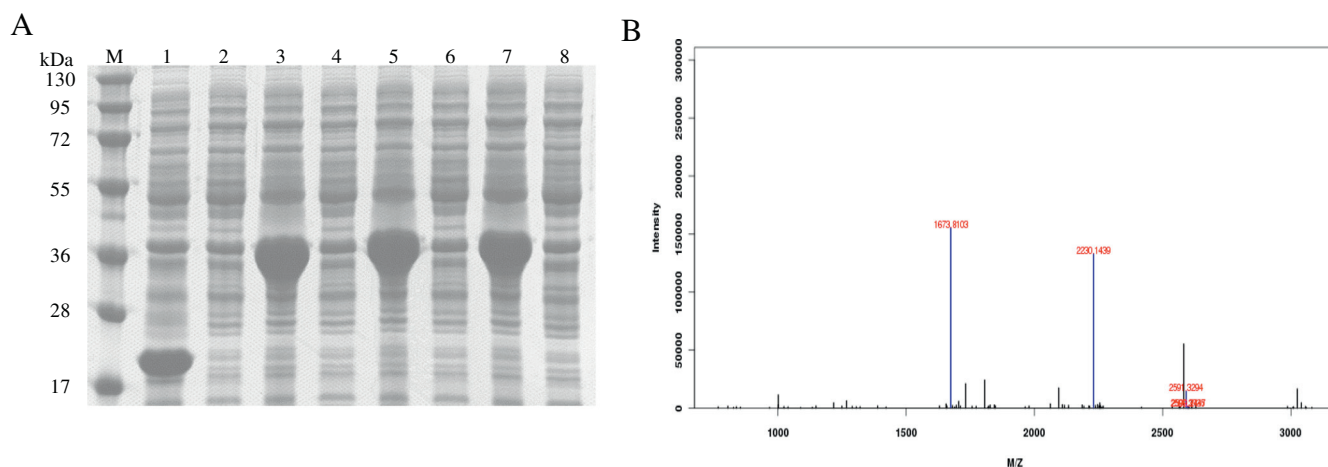


**Fig. 2.** SDS-PAGE analysis of Xyn2 and mass spectrometry. (A) M: Mark; Lanes 1, 3, 5, 7: The total protein of *E. coli* Origami containing pET32a, pET32a-Xyn2, pET32a-Xyn2<sup>C14–52</sup>, and pET32a-Xyn2<sup>C59–149</sup> induced with 0.1% IPTG. Lane 2, 4, 6, 8: The total protein of *E. coli* Origami containing pET32a, pET32a-Xyn2, pET32a-Xyn2<sup>C14–52</sup>, and pET32a-Xyn2<sup>C59–149</sup> that were non-induced. (B) MS results of Xyn2; the blue line indicates that the peak matched and the black line indicates that the peak was unmatched.

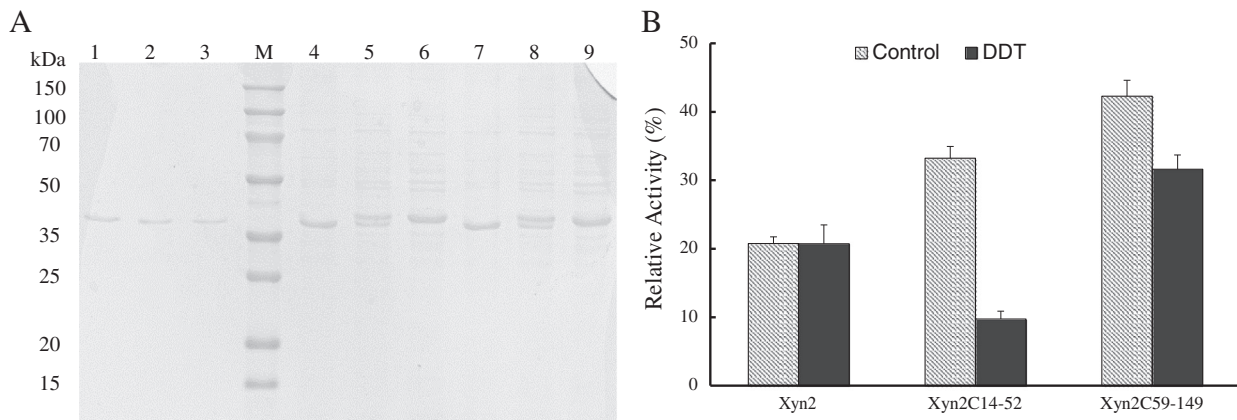


**Fig. 3.** Validation of the disulfide bonds formation. (A) M: Mark; Lanes 1, 2, 3: the wild enzyme not containing a disulfide bond treated with 0, 2.5, and 10 mmol DDT. Lane 4: untreated XYN2<sup>C14-52</sup>; Lane 5: XYN2<sup>C14-52</sup> with 2.5 nmol DDT; Lane 6: XYN2<sup>C14-52</sup> with 10 nmol DDT; Lane 7: untreated XYN2<sup>C59-149</sup>; Lane 8: XYN2<sup>C59-149</sup> with 2.5 mmol DDT; Lane 9: XYN2<sup>C59-149</sup> with 10 mmol DDT. (B) The residual activity of DDT-treated (or not) Xyn2, Xyn2<sup>C14-52</sup>, and Xyn2<sup>C59-149</sup> after incubating at 60°C for 10 min.

thermostability of Xyn2<sup>C14-52</sup> and Xyn2<sup>C59-149</sup> is the result of the formation of disulfide bonds.

### 3.4. Optimal temperature and thermostability

The mutant Xyn2<sup>C59-149</sup> showed the same optimal temperature of 60°C as the wild type Xyn2 but also showed improved activity at temperatures above 60°C (Fig. 4A). All these mutants maintained over 20% relative activity at 75°C, whereas the wild type lost almost all of its activity at this temperature. However, the mutant Xyn2<sup>C14-52</sup> showed lower thermostability than the wild type Xyn2 at temperatures below 60°C, but this activity dropped only 72% when the temperature was increased from 55°C to 75°C (Fig. 4B). Furthermore, the degradation profiles of Xyn2 and its mutants at 60°C showed that Xyn2 and Xyn2<sup>C59-149</sup> degraded at a constant rate,

whereas the mutant Xyn2<sup>C14-52</sup> degraded rapidly for the initial 60% of relative activity but slowly for the final 40% of relative activity (Fig. 4C).

### 3.5. Optimal pH and stability

The pH activity profiles of Xyn2 and its mutants showed a similar trend. All the enzymes had the same optimal pH of 6.0 and showed no significant difference of relative activity in alkali conditions. However, the mutants Xyn2<sup>C14-52</sup> and Xyn2<sup>C59-149</sup> showed approximately 30 and 40% relative activity, respectively, whereas the wild type Xyn2 showed only 20% relative activity (Fig. 5A). All the Xyn2 mutants showed improved stability after incubation at 60°C for 10 min in acidic conditions (pH 2.0–5.0), and the stability of mutant Xyn2<sup>C14-52</sup> increased by over four-fold compared to that of the wild type in the extremely acidic condition (pH 2.0). Furthermore, the mutant

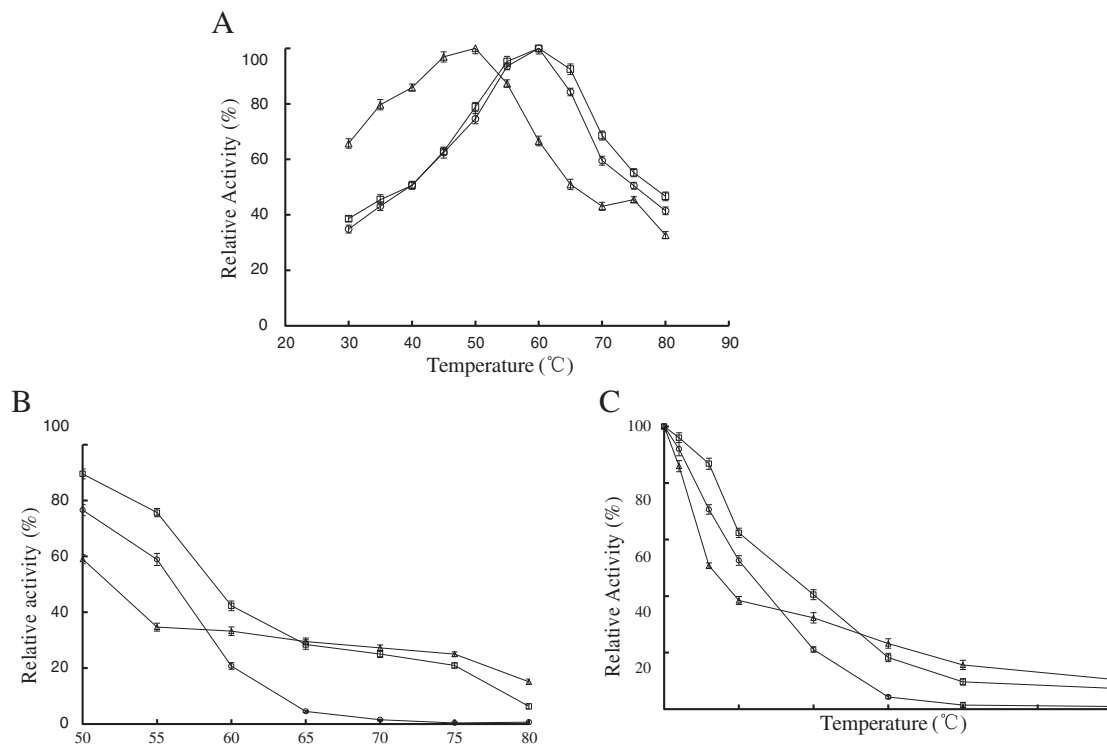


**Fig. 4.** Optimal temperature and thermostability. (A) Relative activity of Xyn2, Xyn2<sup>C14-52</sup>, and Xyn2<sup>C59-149</sup> at each temperature. (B) Relative residual activity after incubation for 10 min at high temperature. (C) Relative residue activity after incubation at 60°C at every indicated time.

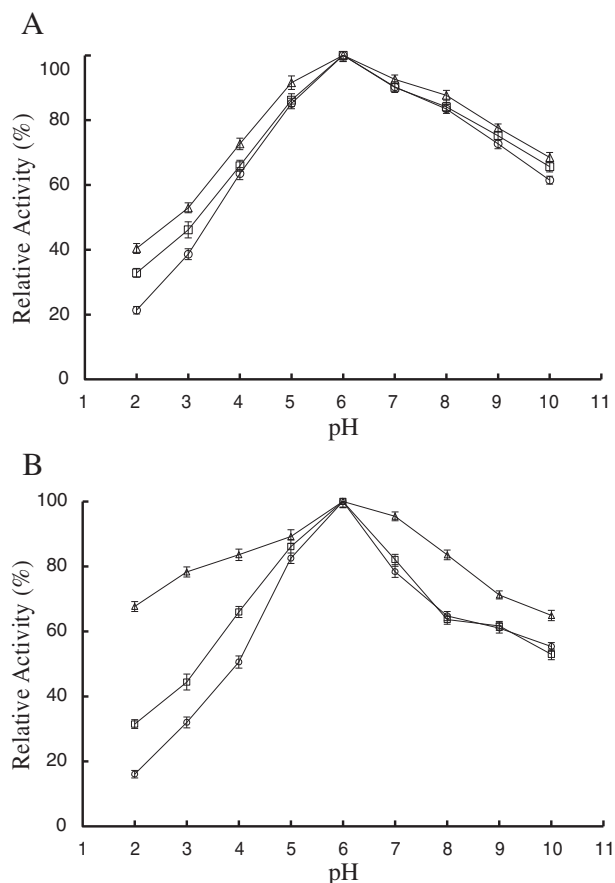


**Fig. 5.** The optimal pH and pH stability. (A) Relative activity of Xyn2, Xyn2<sup>C14-52</sup>, and Xyn2<sup>C59-149</sup> in each pH buffer. (B) Relative residual activity after incubation at 60°C for 10 min in a range of pH from 2 to 10.

Xyn2<sup>C14-52</sup> had better resistance to alkaline conditions (pH 8.0–10.0). However, the mutant Xyn2<sup>C59-149</sup> did not have improved alkali resistance (Fig. 5B).

### 3.6. Kinetic parameters

The catalytic activity of the xylanases was demonstrated by the kinetic parameter specific activity; the specific activities of Xyn2, Xyn2<sup>C14-52</sup>, and Xyn2<sup>C59-149</sup> were  $617.31 \pm 20.88$ ,  $313.97 \pm 12.41$ , and  $524.17 \pm 17.08$  U/mg, respectively (Table 2). The results show that the introduction of a disulfide bond has a negative effect on the catalytic activity of xylanase. The substrate binding capacity of xylanases was described by  $K_m$ ; the  $K_m$  values of Xyn2, Xyn2<sup>C14-52</sup>, and Xyn2<sup>C59-149</sup> were 5.9, 18.5, and 5.7, respectively (Table 2). This indicates that the disulfide bond location in the N-terminal negatively affects the substrate binding capacity of xylanase, but the disulfide bond in the  $\alpha$ -helix has no influence on the substrate binding ability. The half-life of the mutants Xyn2<sup>C14-52</sup> and Xyn2<sup>C59-149</sup> at 60°C was 9.6 and 7.1 min, respectively, which were improvements of approximately 2.5- and 1.8-fold, respectively, compared to the wild type of 3.9 min.

## 4. Discussion

Xylanase is one of the most important commercial enzymes that is widely used in industry. However, the application of xylanases is restricted by its inability to cope with various harsh conditions such as high temperatures and extreme acidic and alkaline conditions [2,8]. Many studies on GH family 11 xylanases have reported the introduction of a disulfide bond, which increased the aromatic interaction and other intermolecular forces at the N-terminal or  $\alpha$ -helix, thus efficiently improving the stability of the entire protein [17,20,24,25]. In short, efficient packing of the N-terminal and  $\alpha$ -helix is key to the thermostability of the GH family 11 xylanases. However, the relationships between the N-terminal and  $\alpha$ -helix and the  $\beta$ -sheet core have not yet been elucidated.

In this work, we introduced two disulfide bonds to connect the N-terminal and the  $\alpha$ -helix to the  $\beta$ -sheet core in this study. The disulfide bonds are considered to stabilize the protein structure by decreasing the entropy of the unfolded state. Two of the disulfide bonds separately connected the N-terminal and  $\alpha$ -helix to the  $\beta$ -sheet core in two mutant Xyn2. As a result, the half-lives of the Xyn2<sup>C14-52</sup> and Xyn2<sup>C59-149</sup> mutants were improved at 60°C, indicating that the binding of the N-terminal and  $\alpha$ -helix to the  $\beta$ -sheet core contributes to the stability of the entire protein. Furthermore, the Xyn2<sup>C14-52</sup> and Xyn2<sup>C59-149</sup> mutants retain greater residual activity than the wild type after incubation at 70°C for 10 min. Furthermore, after treatment

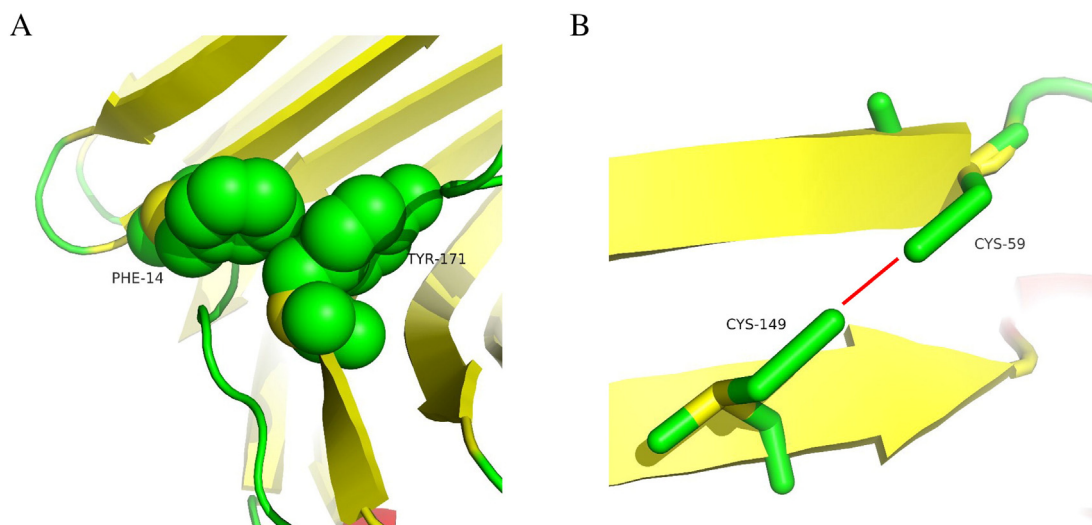


**Fig. 6.** Analysis of the three-dimensional structure. (A) The residues (Phe<sup>14</sup> and Tyr<sup>171</sup>) represented by spheres form an aromatic interaction in wild type. (B) The residues (Cys<sup>59</sup> and Cys<sup>149</sup>) represented with stick form a hydrogen bond in DDT-treated Xyn2<sup>59-149</sup>.

**Table 3**  
Comparison of enzymatic properties of Xyn2, Xyn2<sup>C14–52</sup>, and Xyn2<sup>C59–149</sup>.

Enzymatic properties <sup>a</sup>	Xyn2	Xyn2 <sup>C14–52</sup>	Xyn2 <sup>C59–149</sup>
Optimum temperature (°C)	60	50	60
Optimum pH	6	6	6
pH stability <sup>b</sup>	4–10	2–10	4–10
Specific activity (U/mg)	617.31 ± 20.88	313.97 ± 12.41	524.17 ± 17.08
t <sub>1/2</sub> at 60°C (min)	3.9	9.6	7.1
K <sub>m</sub> (mg/mL)	5.9	18.5	5.7

<sup>a</sup> All the enzymes were diluted to a similar concentration for enzymatic properties analysis and measured in triplicate.

<sup>b</sup> pH range in which residual activity was above 50% relative to the highest residual activity after incubating at 60°C for 10 min.

with 10 mM DDT at 4°C for 12 h, the mutants showed a significant decrease ( $P < 0.05$ ) in residual activity compared to that in the untreated mutants for the same condition, and the wild type enzyme showed no significant difference ( $P > 0.1$ ). This indicates that the disulfide bond plays an important role in connecting the N-terminal and  $\alpha$ -helix to the  $\beta$ -sheet core. This is similar to the packaging of the N-terminal [31]. However, the residual activity of the DDT-treated Xyn2<sup>C59–149</sup> significantly increased ( $P > 0.05$ ) and that of DDT-treated Xyn2<sup>C14–52</sup> significantly decreased ( $P < 0.05$ ) compared to the residual activity of DDT-treated Xyn2 (wild type) for the same condition. The DDT-treated Xyn2<sup>C14–52</sup>, Xyn2<sup>C59–149</sup>, and Xyn2 were modeled by the Protein Interactions Calculator server (Indian Institute of Science, Bangalore, India; <http://pic.mbu.iisc.ernet.in/job.html>) and visualized by the Swiss model program (<http://spdbv.vital-it.ch>). The results showed that there is an extra aromatic interaction in Xyn2 (Fig. 6A) and the presence of a hydrogen bond in Xyn2<sup>C59–149</sup> (Fig. 6B), which is considered to have a similar role as the disulfide bond that connects the N-terminal and  $\alpha$ -helix to the  $\beta$ -sheet core. Similar to the previous study, the packaging of the N-terminal and  $\alpha$ -helix to the  $\beta$ -sheet core has the same effect as the packaging of the N-terminal and the  $\alpha$ -helix themselves [17,23,24,31,32].

In addition, the introduction of the disulfide bond in this work has shown a great improvement in alkali resistance, similar to that in the previous study [24]. Moreover, the introduction of the disulfide bond between the N-terminal and  $\beta$ -sheet core has improved the acid resistance, which has been barely achieved in previous studies.

However, these mutants containing disulfide bonds may be less flexible, which correlates to their decreased specific activities [24]. Moreover, the N-terminal was the most relevant to the catalytic- and substrate-binding capacity of GH family 11 xylanases [33]. Thus, the activity and  $k_m$  of Xyn2<sup>C14–52</sup> were influenced a lot by the introduction of the disulfide bond at the N-terminal (Table 3). However, there was no significant difference of  $k_m$  between the mutant Xyn2<sup>C59–149</sup> and the wild type. The mutant Xyn2<sup>C59–149</sup> lost 15% of its enzyme activity compared to Xyn2, whereas the mutant Xyn2<sup>C14–52</sup> lost almost 50% of its enzyme activity (Table 3).

## 5. Conclusion

In this work, we successfully introduced two disulfide bonds in *T. reesei* xylanase 2 and produced mutant xylanases in *E. coli*. All the mutant xylanases were effective in preventing the unfolding of Xyn2. The packaging of the N-terminal and  $\alpha$ -helix to the  $\beta$ -sheet core by a disulfide bond had the same effect as packaging the N-terminal and  $\alpha$ -helix themselves for improving the stability of GH family 11 xylanases, which may encourage potential ideas for improving the GH family 11 xylanases in the next study. Moreover, packaging the N-terminal and  $\alpha$ -helix to the  $\beta$ -sheet core seems a more efficient method to confer resistance to alkaline and acidic conditions compared to the previous study in which the N-terminal and  $\alpha$ -helix were packaged themselves. However, most of the studies including this work indicate that the N-terminal was the most

relevant to the catalytic- or substrate-binding capacity of the GH family 11 xylanases [33]. Modification in the N-terminal is commonly associated with decrease in activity and substrate-binding capacity [19]. Moreover, some C-terminal modification, including those in this work (Xyn2<sup>C59–149</sup>), has a little or even no influence on the enzyme activity [20]. Thus, more attention should be paid to the C-terminal of GH family 11 in the future.

## Conflict of interest

The authors declare no financial or commercial conflict of interest.

## Financial support

This work was supported by the Fok Ying Tung Education Foundation (no. 141027) and the “Prominent Young Scientist Fund” of Sichuan Province (2013JQ0039).

## Supplementary data

Supplementary data to this article can be found online at <http://dx.doi.org/10.1016/j.ejbt.2017.01.001>.

## References

- Beg Q, Kapoor M, Mahajan L, Hoondal G. Microbial xylanases and their industrial applications: A review. *Appl Microbiol Biotechnol* 2001;56:326–38. <http://dx.doi.org/10.1007/s002530100704>.
- Motta FL, Andrade CC, Santana MHA. A review of xylanase production by the fermentation of Xylan: Classification, characterization and applications. In: Anuj C, editor. Sustainable degradation of lignocellulosic biomass – Techniques, applications and commercialization. InTech; 2013. <http://dx.doi.org/10.5772/53544>.
- Kumar PR, Eswaramoorthy S, Vithayathil PJ, Viswamitra MA. The tertiary structure at 1.59 Å resolution and the proposed amino acid sequence of a family-11 xylanase from the thermophilic fungus *Paecilomyces varioti* Bainier. *J Mol Biol* 2000;295:581–93. <http://dx.doi.org/10.1006/jmbi.1999.3348>.
- Gruber K, Klintschar G, Hayn M, Schlacher A, Steiner W, Kratky C. Thermophilic xylanase from *Thermomyces lanuginosus*: High-resolution X-ray structure and modeling studies. *Biochemistry* 1998;37:13475–85. <http://dx.doi.org/10.1021/bi980864l>.
- Margeot A, Hahn-Hagerdal B, Edlund M, Slade R, Monot F. New improvements for lignocellulosic ethanol. *Curr Opin Biotechnol* 2009;20:372–80. <http://dx.doi.org/10.1016/j.copbio.2009.05.009>.
- Butt MS, Tahir-Nadeem M, Ahmad Z, Sultan MT. Xylanases and their applications in baking industry. *Food Technol Biotechnol* 2008;46:22–31.
- Verma D, Satyanarayana T. Molecular approaches for ameliorating microbial xylanases. *Bioresour Technol* 2012;117:360–7. <http://dx.doi.org/10.1016/j.biortech.2012.04.034>.
- Paes G, Berrin JG, Beaugrand J. GH11 xylanases: Structure/function/properties relationships and applications. *Biotechnol Adv* 2012;30:564–92. <http://dx.doi.org/10.1016/j.biotechadv.2011.10.003>.
- Sharma A, Adhikari S, Satyanarayana T. Alkali-thermostable and cellulase-free xylanase production by an extreme thermophile *Geobacillus thermoleovorans*. *World J Microbiol Biotechnol* 2007;23:483–90. <http://dx.doi.org/10.1007/s11274-006-9250-1>.
- Satyanarayana DV. Improvement in thermostability of metagenomic GH11 endoxylanase (Mxyl) by site-directed mutagenesis and its applicability in paper pulp bleaching process. *J Ind Microbiol Biotechnol* 2013;40:1373–81. <http://dx.doi.org/10.1007/s10295-013-1347-6>.
- Vogl T, Brengelmann R, Hinz HJ, Scharf M, Lötzbeyer M, Engels JW. Mechanism of protein stabilization by disulfide bridges: Calorimetric unfolding studies on disulfide-deficient mutants of the  $\alpha$ -amylase inhibitor tandemistat. *J Mol Biol* 1995;254:481–96. <http://dx.doi.org/10.1006/jmbi.1995.0632>.
- Sunna A, Bergquist PL. A gene encoding a novel extremely thermostable 1,4- $\beta$ -xylanase isolated directly from an environmental DNA sample. *Extremophiles* 2003;7:63–70. <http://dx.doi.org/10.1007/s00792-002-0296-1>.
- Ruller R, Alponi J, Deliberto LA, Zaphorlin LM, Machado CB, Ward RJ. Concomitant adaptation of a GH11 xylanase by directed evolution to create an alkali-tolerant/thermophilic enzyme. *Protein Eng Des Sel* 2014;27:255–62. <http://dx.doi.org/10.1093/protein/gzu027>.
- Imani M, Hosseinkhani S, Ahmadian S, Nazari M. Design and introduction of a disulfide bridge in firefly luciferase: Increase of thermostability and decrease of pH sensitivity. *Photochem Photobiol Sci* 2010;9:1167–77. <http://dx.doi.org/10.1039/c0pp00105h>.
- Creighton TE. What the papers say: Protein folding pathways determined using disulphide bonds. *Bioessays* 1992;14:195–9. <http://dx.doi.org/10.1002/bies.950140310>.
- Wang WC, Chiu WC, Chen CY, You JY. Increasing thermostability of N-carbamoyl-D-amino acid amidohydrolase by introducing additional intermolecular disulfide

- bridges. *Acta Crystallogr Sect A Found Crystallogr* 2005;6:330. <http://dx.doi.org/10.1107/S010876730508596X>.
- [17] Zhang S, Zhang K, Chen X, Chu X, Sun F, Dong Z. Five mutations in N-terminus confer thermostability on mesophilic xylanase. *Biochem Biophys Res Commun* 2010;395:200–6. <http://dx.doi.org/10.1016/j.bbrc.2010.03.159>.
- [18] Jun H, Bing Y, Keying Z, Xuemei D, Daiwen C. Thermostable carbohydrate binding module increases the thermostability and substrate-binding capacity of *Trichoderma reesei* xylanase 2. *N Biotechnol* 2009;26:53–9. <http://dx.doi.org/10.1016/j.nbt.2009.04.002>.
- [19] Sun JY, Liu MQ, Xu YL, Xu ZR, Pan L, Gao H. Improvement of the thermostability and catalytic activity of a mesophilic family 11 xylanase by N-terminus replacement. *Protein Expr Purif* 2005;42:122–30. <http://dx.doi.org/10.1016/j.pep.2005.03.009>.
- [20] Joo JC, Pack SP, Kim YH, Yoo YJ. Thermostabilization of *Bacillus circulans* xylanase: Computational optimization of unstable residues based on thermal fluctuation analysis. *J Biotechnol* 2011;151:56–65. <http://dx.doi.org/10.1016/j.jbiotec.2010.10.002>.
- [21] Zhang H, Li J, Wang J, Yang Y, Wu M. Determinants for the improved thermostability of a mesophilic family 11 xylanase predicted by computational methods. *Biotechnol Biofuels* 2014;7:3. <http://dx.doi.org/10.1186/1754-6834-7-3>.
- [22] Yang HM, Meng K, Luo HY, Wang YR, Yuan TZ, Bai YG, et al. Improvement of the thermostability of xylanase by N-terminus replacement. *Chin J Biotechnol* 2006;22:26–32. [http://dx.doi.org/10.1016/S1872-2075\(06\)60003-4](http://dx.doi.org/10.1016/S1872-2075(06)60003-4).
- [23] Wang Y, Fu Z, Huang H, Zhang H, Yao B, Xiong H, et al. Improved thermal performance of *Thermomyces lanuginosus* GH11 xylanase by engineering of an N-terminal disulfide bridge. *Bioresour Technol* 2012;112:275–9. <http://dx.doi.org/10.1016/j.biortech.2012.02.092>.
- [24] Yang HM, Yao B, Meng K, Wang YR, Bai YG, Wu NF. Introduction of a disulfide bridge enhances the thermostability of a *Streptomyces olivaceoviridis* xylanase mutant. *J Ind Microbiol Biotechnol* 2007;34:213–8. <http://dx.doi.org/10.1007/s10295-006-0188-y>.
- [25] Ayadi DZ, Sayari AH, Hlima HB, Mabrouk SB, Mezghani M, Bejar S. Improvement of *Trichoderma reesei* xylanase II thermal stability by serine to threonine surface mutations. *Int J Biol Macromol* 2015;72:163–70. <http://dx.doi.org/10.1016/j.jbiomac.2014.08.014>.
- [26] Törrönen A, Mach RL, Messner R, Gonzalez R, Kalkkinen N, Harkki A, et al. The two major xylanases from *Trichoderma reesei*: Characterization of both enzymes and genes. *Nat Biotechnol* 1992;10:1461–5. <http://dx.doi.org/10.1038/nbt1192-1461>.
- [27] Kulkarni N, Shendye A, Rao M. Molecular and biotechnological aspects of xylanases. *FEMS Microbiol Rev* 1999;23:411–56. <http://dx.doi.org/10.1111/j.1574-6976.1999.tb00407.x>.
- [28] Wan J, Li Y, Chen D, Yu B, Zheng P, Mao X, et al. Expression of a tandemly arrayed plectasin gene from *Pseudoplectania nigrella* in *Pichia pastoris* and its antimicrobial activity. *J Microbiol Biotechnol* 2016;26:461–8. <http://dx.doi.org/10.4014/jmb.1508.08091>.
- [29] Zhang H, Wu M, Li J, Gao S, Yang Y. Cloning and expression of a novel xylanase gene (*Auxyn11D*) from *Aspergillus usami* E001 in *Pichia pastoris*. *Appl Biochem Biotechnol* 2012;167:2198–211. <http://dx.doi.org/10.1007/s12010-012-9757-x>.
- [30] Wakarchuk WW, Sung WL, Campbell RL, Cunningham A, Watson DC, Yaguchi M. Thermostabilization of the *Bacillus circulans* xylanase by the introduction of disulfide bonds. *Protein Eng Des Sel* 1994;11:1379–86. <http://dx.doi.org/10.1093/protein/7.11.1379>.
- [31] Fenel F, Leisola M, Jänis J, Turunen O. A de novo designed N-terminal disulphide bridge stabilizes the *Trichoderma reesei* endo-1,4- $\beta$ -xylanase II. *J Biotechnol* 2004;108:137–43. <http://dx.doi.org/10.1016/j.jbiotec.2003.11.002>.
- [32] Le QAT, Joo JC, Yoo YJ, Kim YH. Development of thermostable *Candida antarctica* lipase B through novel in silico design of disulfide bridge. *Biotechnol Bioeng* 2012;109:867–76. <http://dx.doi.org/10.1002/bit.24371>.
- [33] Liu Q, Wang Y, Luo H, Wang L, Shi P, Huang H, et al. Isolation of a novel cold-active family 11 xylanase from the filamentous fungus *Bispora antennata* and deletion of its N-terminal amino acids on thermostability. *Appl Biochem Biotechnol* 2015;175:925–36. <http://dx.doi.org/10.1007/s12010-014-1344-x>.